

Supporting information for

facile, continuous and large-scale synthesis of CL-20/HMX nano co-crystals with high-performance by ultrasonic spray-assisted electrostatic adsorption method

Bing Gao,[†] Dunju Wang,[†] Juan Zhang, Yingjie Hu, Jinpeng Shen, Jun Wang, Bing Huang, Zhiqiang Qiao, Hui Huang, Fude Nie* and Guangcheng Yang*

Contents

- ESI 1. Experimental apparatus illustration**
- ESI 2. Powder X-ray Diffraction of CL-20/HMX nano crystals**
- ESI 3. Raman Spectroscopy**
- ESI 4. Particle size distribution**
- ESI 5. Hydrogen bonding analysis**
- ESI 6. Powder X-ray Diffraction CL-20/NTO nano crystals**
- ESI 7. FE-SEM image of CL-20/NTO nano crystals**
- ESI 8. References**

ESI 1. Experimental section

Caution: CL-20 and HMX are both dangerous high explosives. Unexpected misoperation was discouraged during this work. Proper safety practices and equipment must be used to prevent explosion due to friction, heat, static shock, or impact. Be aware of the fact that the potential for severe injury exists if these materials are improperly handled.

Apparatus illustration

The ultrasonic spray-assisted electrostatic experimental installation which was designed by our own laboratory is shown in Fig. S1. There are three main components: (1) ultrasonic spray. It is used to generate an aerosol on the upper liquid surface of the solution and (2) an oven which is heated differently with different zones. The half of the oven close to the entry is in hot surroundings with a maximum temperature of 90-120°C and attenuate to 60-80°C towards the other half of the oven. The oven is heated by the heater band which tightly bound around the oven. (3) Electrostatic adsorption precipitator composed of two electrodes between which an electrostatic field would be existing once the switch turned on. According to security consideration and balancing the efficiency of the installation, the minimum distance of the two electrodes is not less than 9.0 cm. When ultrasonic spray is turned on, aerosols are produced on the upper of the solution, the aerosols quantity is affected by the frequency as well as the liquid level, then the aerosols are transported by the inert gas (nitrogen) towards the container and turn into droplets.

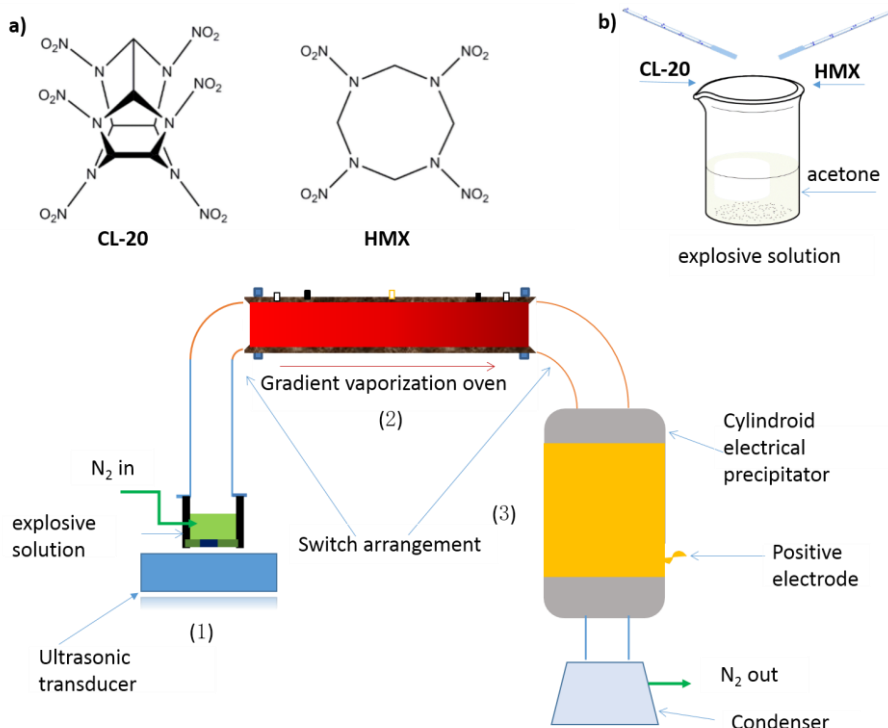


Fig. S1 A brief representation of the apparatus for nano co-crystals by UESA method.

ESI 2. Powder X-ray Diffraction

The phase content of sample was determined by Powder X-ray diffraction (PXRD, X'Pert Pro, PANalytical, The Netherlands) analysis using Cu-K α ($\lambda = 1.540598 \text{ \AA}$) radiation at 50 kV and 30 mA and a graphite diffracted-beam monochromatic. The samples were packed into an amorphous silicon holder and the diffraction angle (2θ) scanned from 5 to 80 $^{\circ}$; The scanning rate was 10 min $^{-1}$. Powder patterns were processed using X'pert highscore Plus^[1] to calculate peak positions, intensities and FWHM.

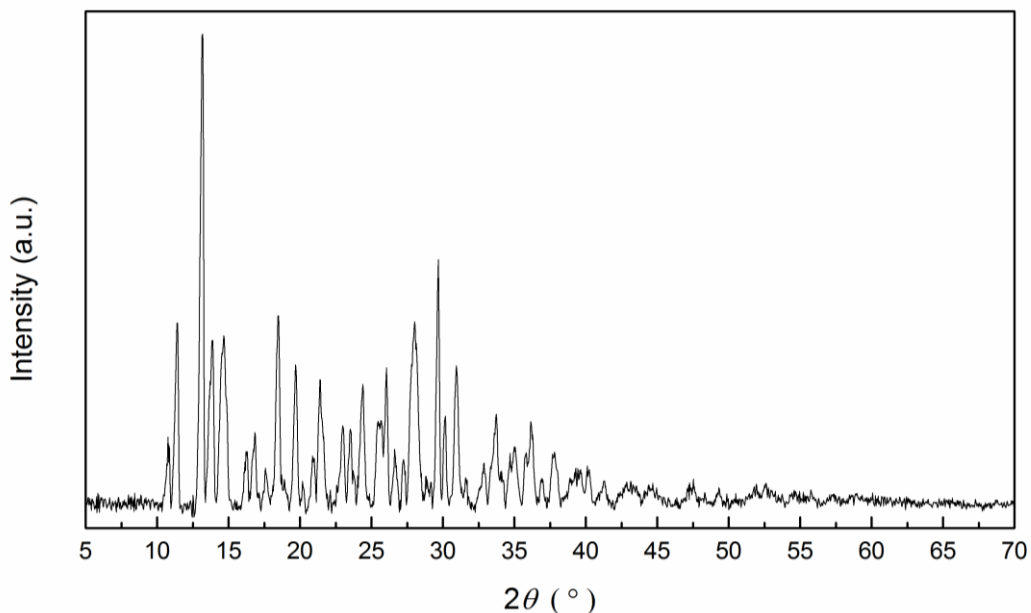


Fig. S2 Individual PXRD pattern of co-crystal **CL-20/HMX**.

Tab. S1 Experimental PXRD peak position and the relative intensity of co-crystal **CL-20/HMX**.

2θ (°)	I/I_0 (%)	FWHM (°)	2θ (°)	I/I_0 (%)	FWHM (°)
5.10	2.47	0.13	28.19	32.74	0.45
10.75	15.74	0.26	28.86	5.05	0.19
11.42	33.22	0.29	29.67	46.96	0.26
13.14	100	0.30	30.08	23.25	0.29
13.88	40.18	0.26	30.92	27.97	0.39
14.56	38.14	0.32	31.66	3.69	0.19
14.81	25.91	0.58	32.97	5.54	0.26
15.39	0.65	0.09	33.30	6.41	0.16
16.22	13.13	0.32	33.71	14.66	0.26
16.80	17.25	0.26	34.11	9.27	0.18
17.20	0.91	0.09	34.65	9.43	0.19
17.69	5.18	0.23	35.15	2.58	0.26
18.47	35.83	0.32	35.71	7.10	0.16
18.87	2.46	0.13	36.28	7.74	0.32
19.65	28.45	0.39	36.87	2.77	0.13
20.27	7.15	0.23	37.66	5.85	0.26
20.91	10.91	0.23	37.97	10.71	0.19
21.35	25.54	0.26	39.03	5.8	0.52
22.14	1.47	0.16	39.60	7.57	0.19
22.98	18.42	0.26	40.19	8.19	0.23
23.00	17.65	0.25	41.32	5.29	0.23
23.47	17.47	0.26	42.49	3.08	0.91
24.37	24.21	0.32	44.77	3.59	0.78
25.36	16.21	0.26	47.56	4.39	0.19
26.06	21.82	0.26	49.39	3.47	0.19
26.76	3.73	0.16	51.90	3.84	0.39
27.12	7.73	0.26	52.45	4.45	0.32
27.66	26.45	0.26	54.49	2.06	0.52

ESI 3. Raman Spectroscopy

Raman spectra were collected using Raman spectroscopy(Raman spectrum, Renishaw,inVia, Britain) equipped with a Leica microscope, RenCam CCD detector632.8 nm laser, 1800 lines/nm grating, and 50 μm slit. Spectra were collected in extended scan mode in the range of 3200-100 cm^{-1} and then analyzed using the LabSpec5.0 software package. Calibration was performed using a silicon standard.

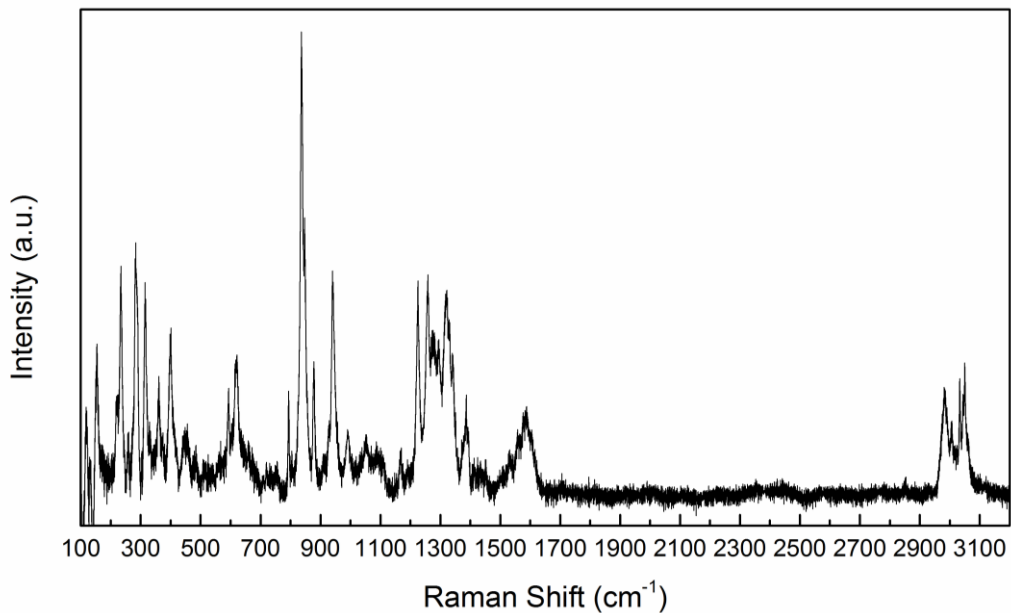


Fig. S3 Individual Raman Spectrum of co-crystal **CL-20/HMX**.

Tab. S2 Frequency of Raman vibrational modes (cm^{-1}) of co-crystal **CL-20/HMX**.

150.77	592.93	1051.56	1411.51
167.88	620.80	1086.06	1423.65
221.19	660.50	1107.93	1434.14
234.02	719.26	1155.05	1451.80
258.43	755.44	1167.67	1508.94
282.84	793.40	1225.73	1532.40
314.71	804.20	1257.70	1560.63
360.22	837.01	1276.21	1588.67
374.08	847.95	1293.88	1606.30
399.58	879.08	1320.80	2982.82
452.37	927.88	1331.74	3008.90
482.02	940.50	1341.83	3044.93
561.50	991.82	1387.27	3053.00

Tab. S3 Crystal data and structure refinement of nano-sized co-crystal **Cl-20/HMX**

Crystal structure of nano-sized co-crystal C/H			
Structural parameters	Parameter values	Structural parameters	Parameter values
Formula	C ₃₂ H ₄₀ N ₆₄ O ₆₄	Crystal system	Monoclinic
Space group	P2 ₁ /c (#14)	Cell Volume (Å ³)	1946.42
a (Å)	16.3455	α (°)	90.00
b (Å)	9.9361	β (°)	90.233
c (Å)	12.1419	γ (°)	90.00

ESI 4. Particle size distribution

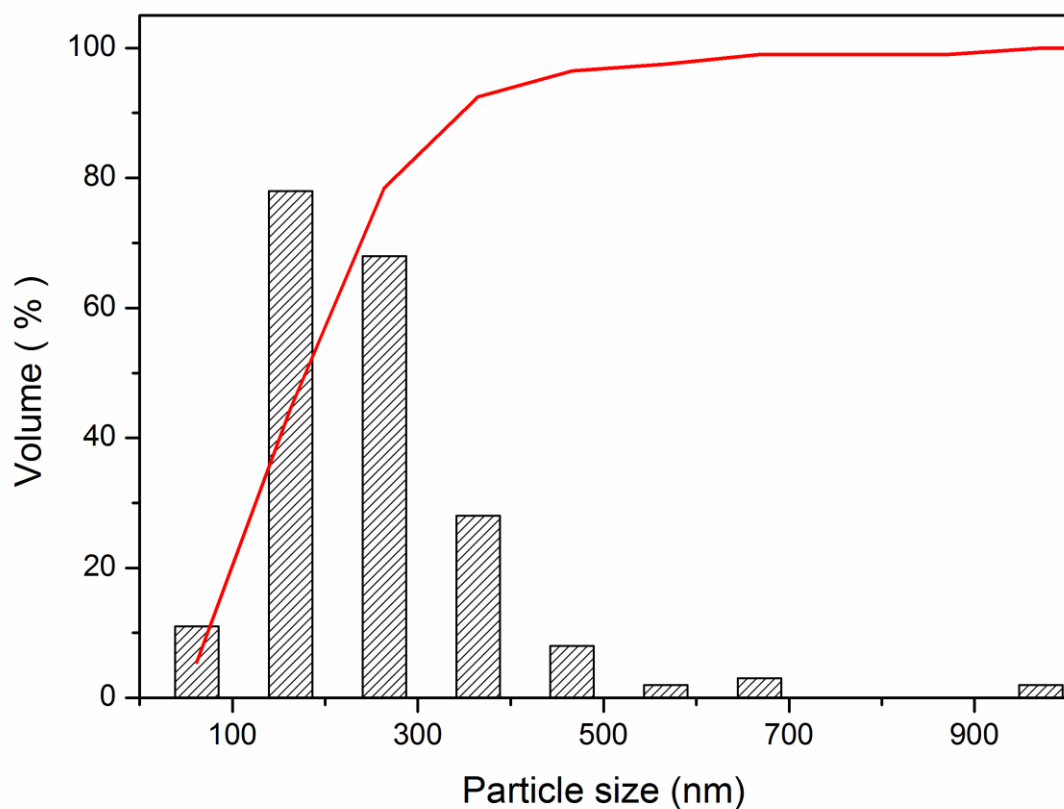


Fig. S4 Particle size and size distribution of co-crystal **CL-20/HMX** measured by dynamic light scattering (DLS).

ESI 5. Hydrogen bonding analysis

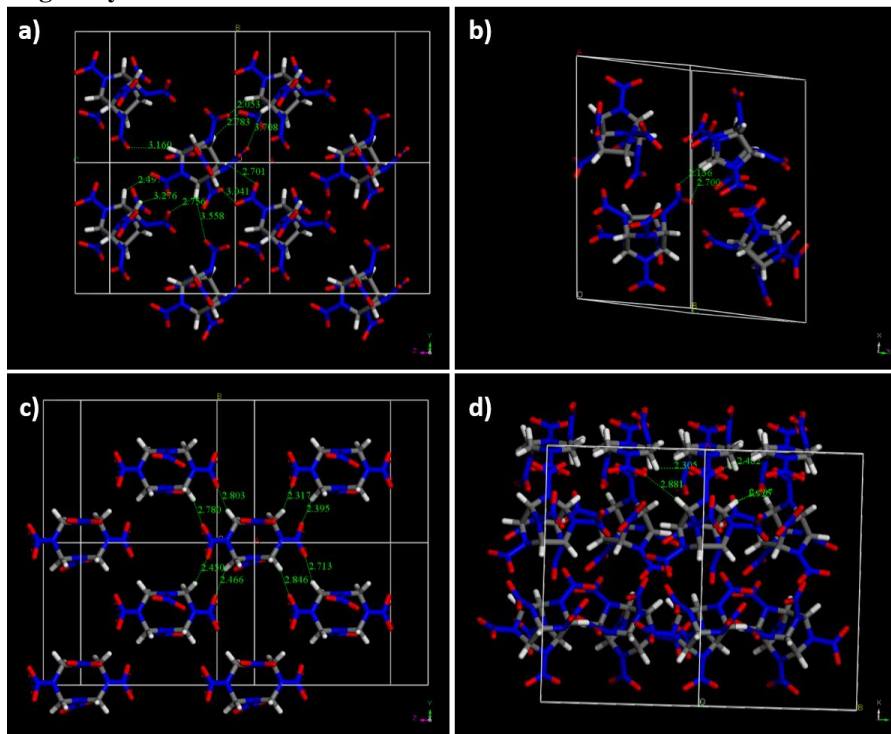


Fig. S5 Hydrogen bonding analysis of co-crystal **CL-20/HMX**, (a) the hydrogen bonding interactions between C-H and nitro group in the same layer of CL-20 molecules, (b) the adjoining hydrogen bonding interactions of CL-20 which appears in pairs and (c) the hydrogen bonding interactions of HMX of co-crystal **CL-20/HMX** (d).

Tab. S4 The bond distances of intermolecular hydrogen bonds found in co-crystal **CL-20/HMX**.

Interaction	d(Å)	Interaction	d(Å)
Same layer molecule in CL-20	2.053	In HMX molecule	2.305
	2.783		2.881
	3.708		2.432
	3.160		2.507
	2.701		1.925
	3.041	In CL-20 adjacent HMX	2.803
	3.558		2.780
	2.756		2.450
	3.276		2.466
	2.497		2.317
Adjacent molecule in CL-20	2.136		2.395
	2.700		2.713
			2.846

ESI 6. Powder X-ray Diffraction CL-20/NTO nano crystals

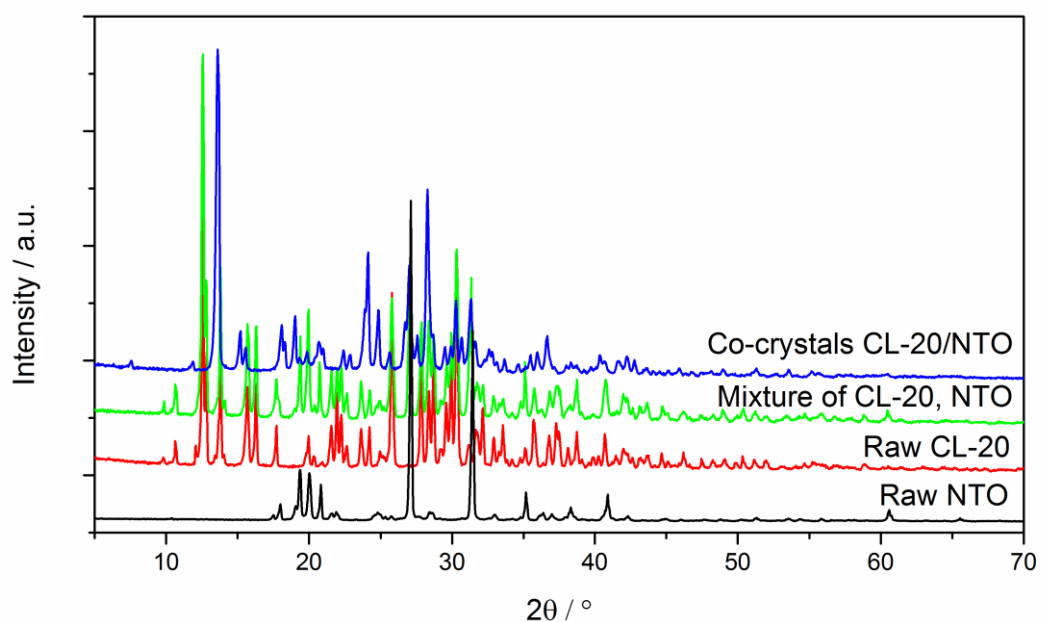


Fig. S6 Comparison of the PXRD patterns of raw NTO, raw CL-20, mixture of the two pure explosives and nano-sized CL-20/NTOcocrystals via ultrasonic spray-assisted electrostatic adsorption (USEA) method.

ESI 7. FE-SEM image of CL-20/NTO nano crystals

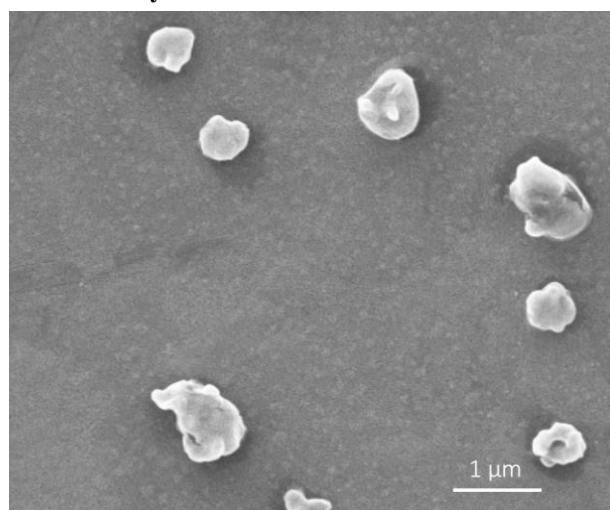


Fig. S7 FE-SEM micrographs of nano-sized cocrystal **CL-20/NTO** by ultrasonic spray-assisted electrostatic adsorption (USA) method.

ESI 8. References

[1] B. PANalytical, *Almelo, The Netherlands* **2006**.